

LA-UR-98-1941

Approved for public release;
distribution is unlimited.

TITLE: EFFECTS OF DYNAMIC JAHN-TELLER DISTORTIONS BY
RAMAN SPECTROSCOPY IN THE LAYERED CMR
MANGANITE LA2-2XSR1+2XMN2O7, X=0.36

CONF-9806136--

AUTHOR(S): H.N. Bordallo, LANSCE 12
D.N. Argyriou, LANSCE 12
J.F. Mitchell, Argonne
G.F. Strouse, UC Santa Barbara

RECEIVED

OCT 05 1998

OSTI

SUBMITTED TO: National Conference on Condensed Matter (ENFMC)
Brazil, 2 June 1998, CAXAMBU-MG

DISTRIBUTION OF THIS DOCUMENT IS UNLIMITED

MASTER

Los Alamos
NATIONAL LABORATORY

Los Alamos National Laboratory, an affirmative action/equal opportunity employer, is operated by the University of California for the U.S. Department of Energy under contract W-7405-ENG-36. By acceptance of this article, the publisher recognizes that the U.S. Government retains a nonexclusive, royalty-free license to publish or reproduce the published form of this contribution, or to allow others to do so, for U.S. Government purposes. The Los Alamos National Laboratory requests that the publisher identify this article as work performed under the auspices of the U.S. Department of Energy. The Los Alamos National Laboratory strongly supports academic freedom and a researcher's right to publish; as an institution, however, the Laboratory does not endorse the viewpoint of a publication or guarantee its technical correctness.

DISCLAIMER

This report was prepared as an account of work sponsored by an agency of the United States Government. Neither the United States Government nor any agency thereof, nor any of their employees, makes any warranty, express or implied, or assumes any legal liability or responsibility for the accuracy, completeness, or usefulness of any information, apparatus, product, or process disclosed, or represents that its use would not infringe privately owned rights. Reference herein to any specific commercial product, process, or service by trade name, trademark, manufacturer, or otherwise does not necessarily constitute or imply its endorsement, recommendation, or favoring by the United States Government or any agency thereof. The views and opinions of authors expressed herein do not necessarily state or reflect those of the United States Government or any agency thereof.

DISCLAIMER

Portions of this document may be illegible in electronic image products. Images are produced from the best available original document.

Effects of Dynamic Jahn-Teller Distortions by Raman Spectroscopy in the Layered CMR Manganite $\text{La}_{2-2x}\text{Sr}_{1+2x}\text{Mn}_2\text{O}_7$, $x=0.36$.

H. N. Bordallo, D. N. Argyriou

Manuel Lujan Jr. Neutron Scattering Center, Los Alamos Nat. Lab. - Los Alamos

J. F. Mitchell

Material Science Division, Argonne National Laboratory - Argonne

G.F. Strouse

Department of Chemistry, University of California - Santa Barbara

The close interplay among charge, spin, and lattice degrees of freedom in the colossal magnetoresistive (CMR) manganite oxides is believed to play an important role in the transport mechanism in these itinerant ferromagnets^{1,2}. While the work on CMR materials has concentrated on the 3D perovskite manganites, the discovery of the layered compounds $\text{La}_{2-2x}\text{Sr}_{1+2x}\text{Mn}_2\text{O}_7$ as another class of CMR oxides provides a rich opportunity to explore the relationship between structure and transport properties on varying length and time scales in reduced dimensions. The crystal structure of the layered CMR compounds $\text{La}_{2-2x}\text{Sr}_{1+2x}\text{Mn}_2\text{O}_7$ is comprised of perovskite bilayers of corner-linked MnO_6 octahedra forming infinite sheets. Doping of divalent cations such as Sr^{2+} gives rise to a mixed valent system where Jahn-Teller (JT) active Mn^{3+} and JT-inactive Mn^{4+} co-exist on the lattice¹⁻⁵. Among the current theoretical models of transport in the three-dimensional perovskite materials is the role of JT. This transport mechanism plays a fundamental role above the Curie temperature (T_C)^{6,7}. Indeed, localized lattice distortions have been observed experimentally above T_C in the $(\text{La,Ca})\text{MnO}_3$ perovskite system.⁸

In this communication, we report resonant Raman spectroscopic measurements on a micro-crystalline sample of $\text{La}_{1.28}\text{Sr}_{1.72}\text{Mn}_2\text{O}_7$ ($x=0.36$). Our measurements suggest discrete phonon modes for the Mn^{3+} and Mn^{4+} lattice sites, which may arise from either dynamic or static localization and the presence of Mn^{2+} defects in the lattice.

Crystals of $\text{La}_{1.28}\text{Sr}_{1.72}\text{Mn}_2\text{O}_7$ were melt-grown in flowing 100% O_2 (balance Ar) in a floating zone optical image furnace (NEC SC-M15HD). From ICP measurements, the composition of the crystals was determined to be consistent with a doping of $x=0.36(1)$. For this material, a paramagnetic insulator (PI) to ferromagnetic metal (FM) transition at 133 K is observed (figure 1).

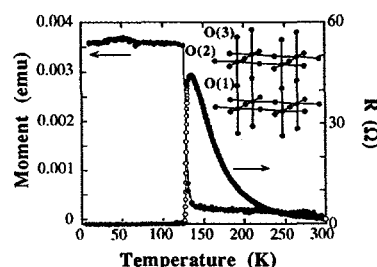


Fig. 1 Magnetization and resistivity of $\text{La}_{1.28}\text{Sr}_{1.72}\text{Mn}_2\text{O}_7$ as a function of temperature. The crystal structure is shown in the inset.

Temperature dependent Raman measurements (488 and 514 nm, 10-20mW) between 300K and 10K were conducted on isotropic samples obtained from a single crystal boule. The samples were cooled in a quartz capillary tube on an APD closed cycle He cryostat to $\pm 5\text{K}$. The temperature dependent evolution of the phonon bands corrected for luminescence is shown in figure 2 ($\lambda = 514 \text{ nm}$). The temperature dependent background will be discussed below.

In figure 2, four distinct sets of phonon bands can be distinguished: 1) a low frequency band below 300 cm^{-1} ; 2) ν_1 and ν_2 between 300 and 580 cm^{-1} ; 3) ν_3 and ν_4 between 600 and 860 cm^{-1} ; and

4) ν_5 , ν_6 and ν_7 between 900 and 1300 cm^{-1} .⁹ Although polarized data is not available, a tentative assignment of the observed Raman bands between 200 and 1000 cm^{-1} can be made based on symmetry considerations and the Mn-O bond lengths.⁴ Correlation of the assigned modes to observations in the temperature dependent neutron diffraction data and to the extensive high T_c superconductor literature is necessary to validate the mode assignments.^{10,11}

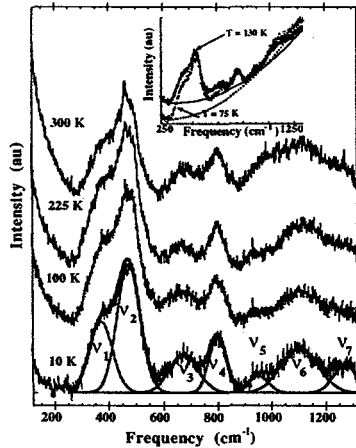


Fig. 2.: Temperature dependent (300-10K) Raman spectra (514nm, 10-20 mW) after background subtraction. The least square fit to seven gaussians are shown for the 10 K spectrum, as well as their sum. "Raw spectra" and background fits at 75 K (dashed line) and 130 K (solid line) are shown in the inset.

For the centrosymmetric, tetragonal $\text{La}_{1.28}\text{Sr}_{1.72}\text{Mn}_2\text{O}_7$ ($I4/mmm - D_{4h}^{17}$, $Z=2$ - see inset of Fig. 1), the phonon modes are determined based upon the site symmetry of the atoms in the tetragonal cell^{4,12,13}. In this particular case, there are 36 degrees of freedom resulting in the following normal modes ($q=0$):

$$\Gamma = 4A_{1g} + 1B_{1g} + 5E_g + 6A_{2u} + 1B_{2u} + 7E_u$$

Of these modes only 10 are Raman active optical phonon modes (A_{1g} , B_{1g} , and E_g), A_{2u} and E_u are infrared active, and B_{2u} is a silent mode^{12,14}. Although, the observed Raman active phonon bands arise from motion of the atoms in the unit cell, assignments of the symmetric modes can be made based upon motion of the O and Mn using the site

symmetry of the atoms in a simplified phonon model^{10-12,14}. A full analysis of the phonon mode model is reserved for a later manuscript, but can be found for similar structures in the superconductor literature¹⁰⁻¹¹. One A_{1g} phonon mode is mainly associated with a symmetric stretch of the O(2) (C_{4v} site) along the c -axis in the tetragonal cell. The other A_{1g} mode is mainly associated with the Mn and O(3) (C_{2v} site) in the ab -plane, giving rise to a pseudo *breathing* type mode¹⁰. Vibrations arising from Mn-O(1) bonds are infra-red active, i.e. u modes which are strictly forbidden in the $A_3\text{Mn}_2\text{O}_7$ structure, and therefore it is reasonable to assume will not have significant intensity in the $(\text{La,Sr})_3\text{Mn}_2\text{O}_7$ structure.

Reported phonon observations in high T_c superconductors indicate the A_{1g} modes dominate the observed Raman spectrum, while the E_g modes are rarely observed. Based upon an assumption of A_{1g} modes, we can tentatively assign (Mn-O(2)) as the lowest frequency mode (ν_1, ν_2), considering the apical Mn-O(2) bond is longer than the equatorial Mn-O(3) bond. The Mn-O(3) mode can then be assigned as (ν_3, ν_4)¹⁵. These assignments are supported by neutron data results showing shorter Mn-O(3) bond distances. A surprising result is the phonon spectrum is the observation of two sets of phonon bands (ν_1, ν_2 and ν_3, ν_4). This may arise from discrete Mn sites in the lattice, which are not observed by neutron diffraction⁴. The assertion of discrete $\text{Mn}^{3+}/\text{Mn}^{4+}$ sites is supported by local structure probes such as pair distribution function (PDF) analysis of diffraction data that suggests a distribution of Mn-O bond lengths due to dynamic JT effects⁸. The frequency for the Mn^{3+} -O stretch should be at lower frequency than the Mn^{4+} due to the larger d-orbital extension of the Mn^{3+} ion. Comparison of assignments of Raman scattering for high T_c superconductors, we tentatively assign ν_1 (371 cm^{-1}) as the Mn^{3+} -O(2) mode, ν_3 (682 cm^{-1}) as the Mn^{3+} -O(3) mode, ν_2

(470 cm^{-1}) as the $\text{Mn}^{4+}\text{-O}(2)$ and ν_4 (803 cm^{-1}) as $\text{Mn}^{4+}\text{-O}(3)$ ^{10,11,15}.

Further support for the above phonon assignment is available by comparing the temperature dependence frequency shifts of the phonon modes to lattice changes in the temperature dependent neutron diffraction data. Above and below T_c , the evolution of the frequency for the phonon bands ($\nu_1\text{-}\nu_4$) follows classical behavior (figure 3). Very close to T_c , the temperature dependence appears to follow a power law.¹⁶ The change in frequency of the ν_1 and ν_3 bands at T_c is not accompanied by the emergence of new Raman modes and suggests an *isostructural* phase transition. The Raman data shows a softening of the apical bands and a hardening of the equatorial bands consistent with an expansion of the $\text{Mn-O}(2)$ bonds and a contraction of the $\text{Mn-O}(3)$ bonds as observed in the neutron experiments.⁴

Accompanying the changes in frequency at T_c there are noticeable changes in the linewidths of the observed Raman modes. Changes in the Raman linewidth with temperature can arise from temperature effects as well as dynamic mobile distortions associated with the hopping of an e_g electron (polarons); JT-active Mn-O bonds that oscillate among several structural minima, will result in an increase in the corresponding bands' linewidth. Above and below T_c , the changes in linewidth show a classical thermal dependence; however, close to T_c the linewidth of the equatorial JT-active $\text{Mn}^{3+}\text{-O}$ shows a rapid increase on cooling to T_c , followed by a decrease below T_c , suggesting a dynamic variation of the $\text{Mn}^{3+}\text{-O}(3)$ site. These Raman measurements indicate that the lattice effects occurring at T_c are due to bond length changes in the coordination sphere of the JT-active Mn^{3+} , in agreement with the strength of the electron-phonon coupling for Mn^{3+} .

The high frequency bands, ν_5 , ν_6 , and ν_7 exhibit a very different temperature dependent behavior than modes $\nu_1\text{-}\nu_4$. The change in the frequency for ν_6 , and ν_7 are inversely correlated and suggests these modes are coupled and degenerate.

A prominent feature in the Raman spectra is a broad background that has two separate contributions (fig. 2): a quasi-elastic, low-frequency ($<200 \text{ cm}^{-1}$) contribution and a broad ($>200 \text{ cm}^{-1}$) contribution shown in the inset for the 75K and 130K spectra. The low frequency ($< 200 \text{ cm}^{-1}$) contribution, which may arise from elastic scattering, exhibits temperature dependence closely correlated to T_c : the intensity is strong in the paramagnetic insulating state and decreases with decreasing temperature into the metallic state, showing little excitation dependence. This intensity may arise from either a soft mode associated with the isostructural phase transition or electronic Raman scattering arising from electron-hole excitations around the Fermi surface^{19,20}. A full analysis of the low frequency Raman spectra by polarized measurements contributions will be given in a later manuscript²¹.

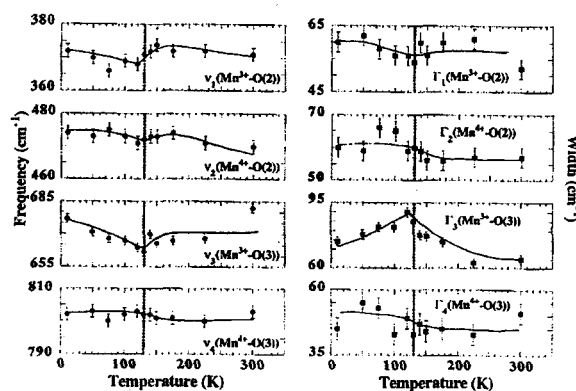


Fig. 3 Temperature dependence of the frequency and linewidth of $\nu_1\text{-}\nu_4$. Dashed line indicates $T_c=133 \text{ K}$.

The broad ($>200 \text{ cm}^{-1}$) background is temperature and excitation dependent. Although electronic Raman modes (2100 cm^{-1}) have been assigned in a similar frequency region for the

perovskite $\text{La}_{0.7}\text{Sr}_{0.3}\text{MnO}_3$, our excitation dependence data indicates the background does not show typical Raman frequency dependence, but rather an excitation independent energy maximum. In conclusion, we believe this background arises from luminescence^{21,23-24}. Based on the fit of the background to a luminescent bandshape ($\lambda_{\text{max}} \sim 690$ nm), the red luminescence in our sample may arise from isolated Mn^{2+} site defects, as has been observed in hexagonal aluminates²⁴. In agreement with our observation, Hundley et al²⁵, has suggested that in the CMR perovskite $\text{La}_{1-x}\text{Sr}_x\text{MnO}_{3+\delta}$ Mn^{2+} defects are present in the lattice that may arise from O deficiencies in the lattice or disproportionation of two Mn^{3+} - Mn^{3+} sites²⁶.

The observed temperature dependence of the optical phonon modes for the layered CMR manganite $\text{La}_{1.28}\text{Sr}_{1.72}\text{Mn}_2\text{O}_7$ is intriguing. The pronounced changes in the frequency of the Mn^{3+} -O band close to T_c reported in this paper demonstrate the significant electron-phonon coupling that accompanies both the electronic and magnetic transitions. Our observations are consistent with a model where JT active Mn^{3+} -O bonds result in the observed lattice anomalies at T_c . The luminescent temperature dependent background observed in the data may be understood in terms of electronically isolated Mn^{2+} defects in the lattice. The observation of two sets of bands for the equatorial and apical modes are tentatively assigned as distinct Mn^{3+} -O and Mn^{4+} -modes in the Raman spectrum. The discrete Mn^{3+} and Mn^{4+} sites in the lattice may arise either from dynamic localization in the lattice (slow electron-hopping rates, $k < 10^{12} \text{ s}^{-1}$) or static localization. The intriguing feature of these measurements is that individual Mn^{3+} and Mn^{4+} cation sites are observed below T_c where a coalescence of the phonon band is expected. It suggests that the length scale and/or hopping frequency of polarons may change below T_c , but that the e_g electron remains largely associated

with the Mn sites within the framework of a large polaron.

The authors thank J. Eckert (Lujan Center, LANL), H. Röder (T-11, LANL) and M. Hundley (MST-10, LANL) for discussions. Work supported by UCSB, and by DOE-BES under contract No. W-7405-ENG-36 and W-31-109-ENG-38.

¹H. Röder, A. Bishop, *Curr. Opin. Sol. State and Mat. Chem.* **2**, 2444 (1997).

²A. Cheetham et al, *Chem. Mater.* **8**, 2421 (1996).

³H. Y. Hwang et al, *PRL.* **75**, 914 (1995).

⁴J. F. Mitchell et al, *PRB B* **55**, 63 (1997).

⁵P. G. Radaelli et al, *PRL.* **75**, 4488 (1995).

⁶A. J. Millis et al, *PRL.* **74**, 5144 (1995).

⁷H. Röder et al *PRL.* **76**, 1356 (1996).

⁸S. J. L. Billinge et al, *PRL.* **77**, 515 (1996).

⁹The 7 band gaussian fitting routine was conducted by linear least squares fitting of the function, $y = K(1) \cdot \exp(-((x-K(2))/K(3))^2)$, using a Levenberg-Marquadt analysis. The fit function was generated by successive iteration of single band fits of $\nu_1 - \nu_7$.

¹⁰V. N. Denisov et al, *PRB* **48**, 16714 (1993).

¹¹M. S. Nair and R. M. P. Jaiswal, *Mater. Sci. Forum.* **405**, 223 (1996).

¹²D. L. Rousseau et al, *J. Raman Spect.* **10**, 253 (1981).

¹³The site symmetries for the atoms in the $(\text{La,Sr})_3\text{Mn}_2\text{O}_7$ lattice are as follows $(\text{La,Sr})_1$ and O_1 D_{4h} , $(\text{La,Sr})_2$, Mn and O_2 C_{4v} , and O_3 C_{2v} .

¹⁴The unit cell is body centered tetragonal, so it contains twice as many atoms as the primitive cell. There are then only 12 atoms in the primitive cell and therefore 36 (3N) degrees of freedom.

¹⁵H. Poulet, J-P Mathieu, *Spectres de Vibration et Symetrie des Cristaux*, Gordon & Breach: (1970).

¹⁶M. R. Ibarra et al, *PRL.* **75**, 3541 (1995).

¹⁷K.H. Kimet al, *PRL.* **77**, 1877 (1996).

¹⁸H. Röder, personal communication.

¹⁹R. Nemetschek et al, *PRL.* **78**, (1997).

²⁰G. Blumberg et al, *PRL.* **78**, 2461 (1997).

²¹H.N. Bordallo et al, *in preparation*.

²²R. Gupta et al, *PRB B* **54**, 14899 (1996).

²³A.L.N. Stevels, *J. Lumin.* **20**, 99 (1979).

²⁴M. F. Hundley and J. J. Neumeier, *PRB* **55**, 11511 (1997).

²⁵J.A.M.V. et al, *J. Sol. State. Chem.* **110**, 106 (1994).